N73-17498

UAH Research Report No. 122

Interim Report

Contract No. NAS8-25750

THE RESPONSES OF THE THERMOSPHERE DUE TO A GEOMAGNETIC STORM - A MHD MODEL

by

S. T. Wu

and

Shih-chih Chang

Submitted by

School of Graduate Studies and Research
The University of Alabama in Huntsville
Post Office Box 1247
Huntsville, Alabama

December 1972

UAH Research Report No. 122

Interim Report

Contract No. NAS8-25750

THE RESPONSES OF THE THERMOSPHERE DUE TO A GEOMAGNETIC STORM - A MHD MODEL

by

S. T. Wu

and

Shih-chih Chang

Submitted by

School of Graduate Studies and Research
The University of Alabama in Huntsville
Post Office Box 1247
Huntsville, Alabama

December 1972

ACKNOWLEDGMENT

This work was supported by Marshall Space Flight Center/NASA under Contract NAS8-25750 with the technical coordination of Mr. R. E. Smith, Chief, Space Environment Branch/Aero-Astronautics Lab. His encouragement and consultation during the course of this study are highly appreciated.

TABLE OF CONTENTS

LIST OF FIGURES

SUMMARY

Magnetohydrodynamics theory has been used to study the dynamic response of the neutral atmosphere to a geomagnetic storm. A full set of magnetohydrodynamic equations appropriate for the present problem is derived and their various orders of approximation are discussed in some detail. In order to demonstrate the usefulness of this theoretical model, the May 1967 geomagnetic storm data recorded at College, Alaska; Dallas, Texas; and Honolulu, Hawaii have been used in the resulting set of non-linear, time dependent, partial differential magnetohydrodynamic equations to calculate variations of the thermosphere due to the storm. The numerical results are presented for wind speeds, electric field strength, and amount of joule heating at a constant altitude for the data recorded at the above-mentioned stations. They show that the strongest thermospheric responses are at the polar region (i.e., College, Alaska), becoming weaker in the equatorial region (i.e., Honolulu, Hawaii). This may lead to the speculation that a thermospheric wave is generated in the polar region due to the geomagnetic storm which propagates towards the equator.

CHAPTER I.

INTRODUCTION

A geomagnetic storm is a natural disturbance of the geomagnetic field on and above the earth's surface. Its origin and associated phenomena are very complicated. Theoretically, a variation of the magnetic field may be caused by the following reasons: 1) variation of the geomagentic poles, 2) presence of local nonhomogeneous electric field $\frac{\partial \vec{B}}{\partial t} = - \nabla \times \vec{E}$, and 3) variation of electric currents.

The magnetic field generated by the earth's magnetic poles is relatively steady. Its variation is negligible in the period of a geomagnetic storm. On the surface of the earth the effect of the ionization of the atmosphere is small and there is no significant electrical field that can be detected. Therefore, it is believed that the geomagnetic disturbance recorded on the earth's surface is mainly due to the existence and variation of electric currents flowing above the earth (Chapman and Bartel [1]). Indeed, if the electric currents data were given for the whole environment of the earth, then the magnetic field could be calculated everywhere, at least theoretically. This would explain the disturbance of the magnetic field recorded on the earth's surface during the geomagnetic storm. Actually, there are always electric currents flowing above the earth, and their intensity and directions are changing from time to time. As a consequence, the geomagnetic field values recorded on the earth will never be constant. If the transient geomagnetic field variations are smooth and regular, we say it is quiet; otherwise it is described as disturbed.

On a quiet day, the magnetic variation proceeds mainly according to local solar time with a small part related to the moon. The two parts are called solar daily and lunar daily magnetic variations, and their correspondence to magnetic fields is denoted by Sq and L. During a magnetic disturbance, additional electric currents flow in the ionosphere. They are superimposed on the Sq and L currents. From the analysis of geomagnetic disturbance data, we see that at least five components of electric currents are involved in a magnetic storm. They are described as follows:

1. DCF = disturbance due to current attributable to solar corpascular flux at magnetopause,
2. DR = disturbance due to magnetic ring current,
3. DP = polar current which is strongest in auroral electrojets,
4. DT = disturbance due to magnetospheric tail currents, and
5. DG = disturbance due to induced ground currents.

Since the electric currents are flowing in the slightly ionized gas medium of the upper atmosphere, the other associated physical and dynamic effects such as wind generation, joule heating, and density and temperature variations can be predicted by magneto-gas-dynamic theory (Piddington [2]). A theoretical feature of the geomagnetic storm and its associated phenomena are illustrated in Diagram I. (See also [2], P. 13.)

Therefore, a complete analysis of the problem of the dynamic structure of the upper atmosphere due to a magnetic storm has to include consideration of the disturbance currents and their associated electric and magnetic fields and the dynamic qualities simultaneously since they are interrelated to each other (see Diagram I). However, the solution of this problem is difficult due to the complexity of the mathematics. Many authors have studied one or a few particular effects separately and made assumptions about the other physical qualities rather arbitrarily; Cole [3] studied the joule heating of moving ionized gas on the assumption of steady and uniform electric and magnetic fields. He concluded that the joule heating effect is significant dueing a geomagnetic storm. The joule heating may be on the otder of 10^{-5} erg cm^{-3} sec^{-1} in the region of 100 to 200 km, and the wind as high as 10^5 cm/sec, if the assumed magnetic and electric field configurations are correct. Later, he [4] extended the results by including viscous effects. Maeda and Kato [5]have given an excellent review on the problems of electrodynamics of the ionosphere in which the problems of conductivity, wind and the dynamo theory, drift and its effect on the ionospheric formation, and the interaction between wind and electromagnetic field are discussed in detail. Thomas [6] and Thomas and Ching [7], applying a one-dimensional vertical model, reproduced the height profile and the mean time lag of the density disturbance by assuring that the heat input due to a magnetic storm is given. Volland and Mayer [8] re-analyzed the same problem using a three-dimensional thermospheric model.

In this study, a theoretical model is established for calculating the joule heating and winds from the geomagnetic variations recorded at storm time. The mathematical formulation is based on the magnetohydrodynamic theory (Chang, Wu, and Smith [9]). Faraday's law is employed for determining the electric field from the magnetic field disturbance data dueing the geomagnetic storm.

CHAPTER II.

FORMULATION OF THE PROBLEM

II-1. Basic Equations

The thermosphere may be considered as a continuum medium with a finite electric conductivity (Cowling [10]). The presence of electric and magnetic fields in the conducting medium will give rise to two principal effects: First, body force (Lorentz force) and, second, energy generation (Joule heating). These must be taken into consideration in the momentum and energy equations. We will derive the equations of mass, momentum, and energy conservation as follows:

Mass Conservation

The equation of mass conservation is the same as in ordinary fluid dynamics, namely

$$\frac{\partial \rho}{\partial t} + \nabla \cdot (\rho \vec{v}) = 0 \tag{1}$$

where ρ denotes the mass density and $\vec{v}$ the velocity vector.

Momentum Conservation

The equation of motion of a continuum medium in general can be written as (Cauchy equation)

$$\rho \frac{D v_i}{D t} = \frac{\partial P_{ij}}{\partial x_j} + F_i \tag{2}$$

where v_i are the components of the velocity vector $\vec{v}$, P_{ij} are components of the stress sensor, and F_i denotes the components of the body force $\vec{F}$. For a Newtonian fluid the stress tensor can be expressed as follows

$$P_{ij} = -p + \frac{2}{3} \eta (\nabla \cdot \vec{v}) \delta_{ij} - \eta \left(\frac{\partial v_i}{\partial x_j} + \frac{\partial v_j}{\partial x_i} \right) \tag{3}$$

where p is the static pressure and η is the viscosity. By substituting Eq. (2) into Eq. (3) we obtain

$$\rho \frac{D \vec{v}}{D t} = - \nabla p + \vec{\chi} + \vec{F} \tag{4}$$

where

$$\vec{\chi} = -\frac{2}{3}\nabla(\eta\,\nabla\cdot\vec{v}) + \eta\,[\nabla^2\vec{v} + \nabla(\nabla\cdot\vec{v})]$$

$$+\ 2\,[((\nabla\eta)\cdot\nabla)\,\vec{v} + (\nabla\eta)\times(\nabla\times\vec{v})]$$

and the body force $\vec{F}$ is

$$\vec{F} = \rho_e\,\vec{E} + \vec{j}\times\vec{B} + \rho\vec{g}$$

where ρ_e is the charge density, $\vec{E}$ is the electric field strength, $\vec{B}$ is the magnetic induction, and $\vec{j}$ is the sum of the conduction current and the current flow due to convective transport of charges.

Energy Conservation

The rate of increase of total energy in the fluid of a moving volume, σ, is given by

$$\int \frac{D\Phi}{Dt}\,d\sigma = \int \frac{1}{2}\,\frac{D(\rho v^2)}{Dt}\,d\sigma + \int \frac{D(\rho e)}{Dt}\,d\sigma\quad.$$

where e is the internal energy per unit mass.

In order for energy to be conserved, this must equal the energy inputs per unit of time from other sources. These are

1. Joule heating $= \int (\vec{E}\cdot\vec{j})\,d\sigma$
2. Heat conduction per unit time $= -\int \nabla\cdot(\lambda\,\nabla T)\,d\sigma$, where λ is the thermal conductivity.
3. Work done by surface force $= -\int \sum_{i,j} v_i\,P_{ij}\,ds_j$ applying Gauss' theorem

$$-\int_S \sum_{i,j} v_i\,P_{ij}\,dS_j = -\int_V \sum_{ij} \frac{\partial}{\partial x_j}(v_i\,P_{ij})\,d\sigma$$

The energy equation is obtained as

$$\int_V \frac{D\Phi}{Dt}\,d\sigma = \int_V \vec{E}\cdot\vec{j}\,d\sigma - \int_V \nabla\cdot(\lambda\,\nabla T)\,d\sigma$$

$$-\int_V \sum_{i,j} \frac{\partial}{\partial x_j}(v_i\,P_{ij})\,d\sigma\quad. \tag{5}$$

The last summation on the right hand side of Eq. (5) can be rewritten as

$$- \sum_i \frac{\partial}{\partial x_i} \left(p\, v_i \right) + \varphi$$

where, from Eq. (3)

$$\varphi = \eta \sum_i v_i \nabla^2 v_i + \frac{1}{3} \eta \sum_i v_i \frac{\partial}{\partial x_i} \left(\sum_j \frac{\partial v_j}{\partial x_j} \right)$$

$$+ \sum_{ij} v_i \frac{\partial \eta}{\partial x_j} \left(\frac{\partial v_i}{\partial x_j} + \frac{\partial v_j}{\partial x_i} \right) + \frac{2}{3} \sum_i v_i \frac{\partial \eta}{\partial x_i} \left(\sum_j \frac{\partial v_j}{\partial x_j} \right)$$

$$+ \eta \sum_{ij} \frac{\partial v_i}{\partial x_j} \left(\frac{\partial v_i}{\partial x_j} + \frac{\partial v_i}{\partial x_i} \right) - \frac{2}{3} \eta \sum_j \left(\frac{\partial v_j}{\partial x_j} \right)^2$$

<u>Maxwell Equations and their Approximation</u>

The Maxwell equations are needed to determine the electromagnetic quantities. Thus,

$$\nabla \cdot \vec{B} = 0 \tag{6}$$

$$\nabla \cdot \vec{E} = \frac{1}{\epsilon} \rho_e \tag{7}$$

$$\nabla \times \vec{E} = - \frac{\partial \vec{B}}{\partial t} \tag{8}$$

$$\nabla \times \vec{B} = \mu_o \left(\vec{J} + \epsilon \frac{\partial \vec{E}}{\partial t} \right) \tag{9}$$

and Ohm's Law;

$$\vec{J} = \sigma \left(\vec{E} + \vec{v} \times \vec{B} \right) + \sigma_2 \left[\vec{B} \times \left(\vec{E} + \vec{v} \times \vec{B} \right) \right] / | \vec{B} | \tag{10}$$

A number of approximations can be made which will be valid as long as the present analysis is concerned:

1) The displacement current $\varepsilon \frac{\partial \vec{E}}{\partial t}$ may be neglected in Eq. (9). In order to show that is a valid approximation, we shall compare $\varepsilon \frac{\partial \vec{E}}{\partial t}$ to the conduction current $J \cong \sigma E$. If E is assumed to vary periodically with time with frequency ω, then the ratio of the amplitude of $\varepsilon\, {}^{\partial E}/_{\partial t}$ to the amplitude of J is approximately

$$\frac{\varepsilon(\partial E/\partial t)\,max}{(\sigma E)\,max} = \frac{\varepsilon\omega}{\sigma} \qquad \frac{\varepsilon\left(\frac{\partial E}{\partial t}\right)_{max}}{(\sigma E)_{max}} = \frac{\varepsilon\omega}{\sigma}$$

The value for σ in our case is about 10^{-3} mhos/m. The value of ε in a vacuum is approximately 9×10^{-12} farads/m. ω is about 10^{-2} sec^{-1}. This gives

$$\frac{\varepsilon\ (\partial E/\partial t)_{max}}{(\sigma E)\,max} \cong 10^{-10}$$

which shows that the displacement current can be indeed neglected.

2) The electrostatic body force

If E varies linearly over some small region, then from Eq. (7) we see

$$\rho_e \cong \frac{\varepsilon E}{L} .$$

Therefore

$$\rho_e E \cong \frac{\varepsilon E^2}{L} .$$

In comparison to the Lorentzian force $J \times B \cong \sigma\, v\, B^2$, we have

$$\frac{\rho_e E}{J \times B} \cong \frac{\varepsilon E^2}{\sigma L v B^2} \cong \frac{\varepsilon v^2 B^2}{\sigma L v B^2} = \frac{\varepsilon v}{\sigma L} .$$

The values in our problem are estimated as follows

$$\varepsilon \cong 10^{-11} \text{ farads/m}$$
$$v \cong 10^{3} \text{ m/sec}$$
$$L \cong 10^{6} \text{ m}$$
$$\sigma \cong 10^{-3} \text{ mhos/m}$$

$$\frac{\varepsilon v}{L \sigma} \cong 10^{-11} .$$

Therefore, the electrostatic body force can be neglected in comparison to the Lorentz force.

Now, let us recollect the above derived equations as follows:

Maxwell's equations:

$$\nabla \times \vec{E} = - \frac{\partial \vec{B}}{\partial t} \tag{11}$$

$$\nabla \times \vec{B} = \mu_o \vec{j} \tag{12}$$

$$\nabla \cdot \vec{B} = 0 \tag{13}$$

$$\epsilon \nabla \cdot \vec{E} = \rho_e \tag{14}$$

Conservation of Mass:

$$\frac{\partial \rho}{\partial t} + \nabla \cdot (\rho \vec{v}) = 0 \tag{15}$$

Equation of Motion:

$$\rho \frac{D \vec{v}}{D t} = - \nabla p + \vec{X} + \vec{j} \times \vec{B} \tag{16}$$

Conservation of Energy:

$$\rho \frac{D \Phi}{Dt} = \vec{E} \cdot \vec{j} + \nabla (\lambda \nabla T) - \nabla \cdot (p \vec{v}) + \varphi \tag{17}$$

Ohm's Law:

$$\vec{j} = \sigma_1 \vec{E}' + \sigma_2 \frac{\vec{B} \times \vec{E}'}{|B|} \tag{18}$$

where $\vec{E}' = \vec{E} + \vec{v} \times \vec{B}$. This set of equations will form the basis of our theoretical analysis. Various approximations will be introduced as long as the physical situations permitt.

II-2. Some Fundamental Solutions

Since the magnetohydrodynamic equations [Eq. (11) - Eq. (18)] combine the full complexity of Maxwell's equations and the fluid dynamic equations, it is obvious that they will be extremely difficult to solve in the general form. Exact solutions exist only for a few special cases. We will discuss two of them; namely, the Piddington [11] solution for a non-viscous gas and the Hartman solution for a viscous fluid [12]. They do not necessarily correspond to the conditions during magnetic storm; however, the solutions will give us some insight into the physical nature of the problem.

(A) Consider a uniform ionized gas in a steady and homogeneous electric field. They are assumed in the following forms

$$\vec{E} = \vec{E}\,(E_x\,,\,E_y,\,0) \quad \text{and} \quad \vec{B} = (0,\,0,\,B_z) \quad .$$

We further assume that the pressure gradient is

$\vec{\nabla} p = \vec{i}\,\frac{\partial p}{\partial x}$, where $\vec{i}$ denotes the unit vector in the x-direction.

By applying Eq. (18) and Eq. (16) and neglecting the viscous term, we obtain

$$\vec{j} = \sigma_1 \vec{E}' + \sigma_2 \frac{\vec{B} \times \vec{E}'}{B_z} \tag{19}$$

and

$$\rho \frac{D\vec{v}}{Dt} = \vec{j} \times \vec{B} - \nabla p \quad . \tag{20}$$

At hydrostatic equilibrium $\frac{D\vec{v}}{Dt} = 0$, then

$$\vec{j} = \frac{-\nabla p \times \vec{B}}{B_z^2} = \sigma_1 \vec{E}' + \sigma_2 \frac{\vec{B} \times \vec{E}'}{B_z} \quad .$$

It follows

$$v_x = E_x / B_z - \frac{\partial p}{\partial x} \Big/ B_z^2 \sigma_3 \;;\; v_y = - E_x / B_z + \frac{\partial p}{\partial x}\sigma_2 \Big/ B_z^2 \sigma_1 \sigma_3 \tag{21}$$

$$j_x = 0 \;, \qquad j_y = \frac{\partial p}{\partial x} \Big/ B_z \tag{22}$$

where $\sigma_3 = \sigma_1 + \sigma_2^2 / \sigma_1$.

Therefore, the current $\vec{j}$ and velocity $\vec{v}$ are solved in terms of $\vec{E}$, $\vec{B}$ and ∇p . The Joule heating is given by

$$Q = \vec{j} \cdot \vec{E}' = \vec{j} \cdot (\vec{E} + \vec{v} \times \vec{B}) \tag{23}$$

This means that if we simulate the mechanism of geomagnetic activity by switching on the electric field $\vec{E}$, after a period of time the velocity, $\vec{v}$, and Joule heating, Q, will reach the values given by Eq. (21) and Eq. (23).

(B) Hartmann Solution

Cole [4] studied the problem of heating and dynamics near auroral electrojets by considering the following model as shown below:

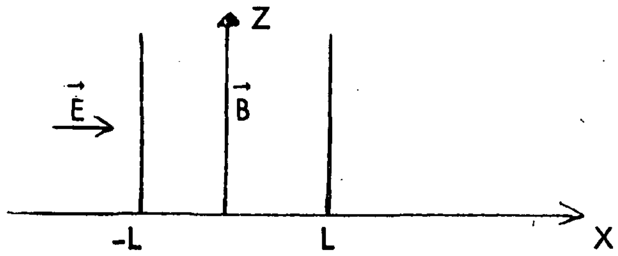

The directions of the electric and magnetic fields are shown in the figure and the direction of flow is perpendicular to x - z plane. If the viscous effect of the fluid is taken into consideration, the momentum equation can be written as:

$$\eta \frac{\partial^2 v_x}{\partial x^2} + \frac{\partial^2 v_y}{\partial z^2} - j_x B = 0 \tag{24}$$

where $j_x = \sigma_1 (E + v_y B_z)$.

Equation (24) can be rewritten as

$$\frac{\partial^2 v_y}{\partial x^2} + \frac{\partial^2 v_y}{\partial z^2} - \frac{\sigma_1}{\mu} |\vec{B}|^2 v_y = \frac{\sigma_2 |\vec{E}| |\vec{B}|}{\eta} \quad . \tag{25}$$

Let us consider the thickness of the sheet of the auroral zone to be 2L and assume that the motion of the gas outside this sheet is small. We can then set the boundary condition as $v_y = 0$ at $x = \pm L$. Then the solution of Eq. (25) that satisfies this boundary condition is given by

$$v_y (x) = \frac{|\vec{E}|}{|\vec{B}|} \left(1 - \frac{\cosh (M_1 x/L)}{\cosh M_1}\right) \tag{26}$$

where $M_1 = |\vec{B}| L (\sigma_{1/\mu})^{\frac{1}{2}}$. The heating within the sheet can be expressed as follows:

$$Q = \eta \left(\frac{|\vec{E}|}{|\vec{B}|} \frac{M_1}{L}\right)^2 \frac{\cosh (M_1 x/L)}{\cosh M_1} \tag{27}$$

II-3. Time Dependent Problem

In the last section we have discussed steady solutions in magneto-gas-dynamics which indeed can help to understand the basic mechanism of Joule heating during a geomagnetic storm. However, they are not sufficient to explain the time variation of the geomagnetic disturbance. Actually all the quantities, electric field, magnetic field and velocity, are time dependent during the entire period of a geomagnetic storm. Therefore, the analysis for the unsteady case is necessary.

Let us recall the equation of motion, namely Eq. (16)

$$\rho \frac{D\vec{v}}{Dt} = - \nabla p + \vec{X} + \vec{j} \times \vec{B} \quad .$$

Suppose that the current data $\vec{j}$ is known (by either observation or theory), then the induced magnetic field may be calculated by Eq. (8), together with the earth magnetic field. Therefore, the last term of Eq. (16) becomes known. The problem is then reduced to a dynamic problem of the atmosphere with an additional given driving force (Lorentz force) and heat source (Joule heating).

On the other hand, if the magnetic field data in the thermosphere are available, we will simplify the problem by eliminating the variables $\vec{E}$ and $\vec{j}$ from the system of equations. This is done by solving Eq. (18), namely,

$$\vec{E} = \frac{\vec{j}}{\sigma_1} - \vec{v} \times \vec{B} + \alpha \; (\vec{j} \times \vec{B}) \quad . \tag{28}$$

where $\alpha = \sigma_2 / \sigma_1^2 \; |\vec{B}|$.

Substitution of $\vec{j}$ from Eq. (12) then gives

$$\vec{E} = \frac{\nabla \times \vec{B}}{\mu_o \sigma_1} - \vec{v} \times \vec{B} + \alpha \quad \frac{\nabla \times \vec{B}}{\mu_o} \times \vec{B} \tag{29}$$

when combined with Eq. (11) gives

$$\frac{\partial \vec{B}}{\partial t} + \nabla \times \frac{\nabla \times \vec{B}}{\mu_o \sigma_1} - \nabla \times (\vec{v} \times \vec{B}) + \nabla \times \frac{\alpha}{\mu_o} (\nabla \times \vec{B}) \times \vec{B} = 0 \; . \tag{30}$$

We notice that Eq. (30) includes only two variables $\vec{B}$ and $\vec{v}$. If $\vec{B}$ (x, y, z, t) is assumed to be given, then the velocity vector can be solved from Eq. (30) with properly imposed boundary conditions.

Equations (11-18) may be reduced in the following form

$$\frac{\partial \rho}{\partial t} + \nabla \cdot (\rho \vec{v}) = 0 \quad , \tag{31}$$

$$\rho \frac{D\vec{v}}{Dt} = -\nabla p + \vec{\chi} + \frac{(\nabla \times \vec{B}) \times \vec{B}}{\mu_o} , \tag{32}$$

$$\rho \frac{D \Phi}{Dt} = \frac{(\nabla \times \vec{B})^2}{\mu_o^2 \sigma} + \nabla \cdot (\lambda \nabla T) - \nabla \cdot (p \vec{v}) + \varphi \, . \tag{33}$$

This set of equations together with Eq. (30) formed a complete description of the time dependent problem. As observed from these equations, the only electromagnetic quantity explicitly involved in this system of equations (30-33) is the magnetic field $\vec{B}$. If $\vec{B}$ is given, this set of equations is reduced to ordinary dynamic equations.

CHAPTER III

NUMERICAL EXAMPLES

III-1. Statement of the Problem

A simplified model considers the thermosphere (80 - 200 KM) as a neutral inviscid atmosphere with finite electric conductivity. Hall effect can be neglected as we have shown in Chapter II. Thus, the set of fundamental equations is as follows:

$$\frac{\partial \rho}{\partial t} + \vec{\nabla} \cdot (\rho \vec{v}) = 0 \tag{34}$$

$$\frac{D\vec{v}}{Dt} = - \frac{1}{p} \vec{\nabla} p + \frac{1}{\rho} (\vec{j} \times \vec{B}) \tag{35}$$

$$\rho C_p \frac{DT}{Dt} = \mathrm{div}\,(\lambda \nabla T) + \vec{j} \cdot \vec{E}' \tag{36}$$

$$\vec{E}' = \vec{E} + \vec{v} \times \vec{B} \tag{37}$$

$$\nabla \times \vec{E} = - \frac{\partial \vec{B}}{\partial t} \tag{38}$$

$$\vec{j} = \sigma (\vec{E} + \vec{v} \times \vec{B}) \tag{39}$$

and

$$p = \rho R T \tag{40}$$

We further assume that the atmospheric motions are confined to the vertical (z - axis) and horizontal (x-axis, E-W) directions. For the magnetic field, since observational data are not available at this stage, we assume quite arbitrarily that

$$\vec{B}(x, y, t) = \vec{b}(t) \exp(-\beta r), \tag{41}$$

where $r = \sqrt{x^2 + y^2}$ and β is an arbitrary constant, which is the measure of the damping rate of geomagnetic variations. This assumed expression for the disturbed geomagnetic variations is such that the maximum disturbance is at the center of the region where we are interested, and it will decay exponentially according to the distance from the center, which also implies that the geomagnetic disturbances are confined in a finite region. Furthermore, the altitude dependence is also ignored in the present study. The quantity $\vec{b}$ (t) is taken from ground station magnetic data. In this calculation the May 1967 geomagnetic storm data recorded at College, Alaska; Dallas, Texas; and Honolulu, Hawaii were used. The 1964 Jacchia model atmosphere was used to calculate the pre-storm conditions of the atmosphere. The set of equations (34-41) was integrated numerically by using a finite difference technique. The numerical process is explained in Diagram (2). It includes the following steps.

1. Calculate $\vec{E}$ from Eq. (38) and (41).
2. Obtain $\vec{E}'$ from Eq. (37).
3. Calculate $\vec{j}$ from Eq. (39).
4. Integrate Eq. (35), determine $\vec{v}$ for next time step, $\vec{v}$ (Δt).
5. Integrate Eq. (36), calculate T (Δt).
6. Calculate p (Δt) from Eq. (40).
7. Determine ρ (Δt) from Eq. (34).
8. Use $\vec{v}$ (Δt) to calculate $\vec{E}'$ (Δt) from Eq. (37).

III-2. Results

Numerical results are presented for winds, joule heating and electric field at the center of the storm and an altitude of 140 KM for May 1967. The calculations are based on the observational data recorded at College, Alaska; Dallas, Texas; and Honolulu, Hawaii. The Alaskan results show that the geomagnetic storm can generate the horizontal wind (East-West direction) (Fig. 4) on the order of maximum 1000 M. sec.$^{-1}$ and vertical wind (Fig. 5) approximately an order of magnitude smaller, which agree with the recent electrojet observation Fees [13]. The joule heating (Fig. 6) is about a few erg -M^{-3} - sec.$^{-1}$ and the electric field (Fig. 3) on the order of 100 mV - M^{-1}, which agree well with the results given by Cole [14] and Wu, Matsushita, and DeVries [15]. However, the calculated temperature in the present model is rather high. We believe this is due to the fact that the present model has not taken into account the effects due to viscosity. Considerably smaller winds, joule heating, and electric field result when the Texas and the Hawaiian data are used instead of the College, Alaska data. The horizontal (East-West) wind v_x over Dallas, Texas (Fig. 10) is calculated to be $\sim$100 M. sec.$^{-1}$ and the vertical wind v_z (Fig 11) is $\sim$10 M. sec^{-1}. The joule heating (Fig. 12) is approximately 10^{-2} erg - M^{-3} - sec.$^{-1}$ and the electric field (Fig. 9) is on the order of 10 mV - M^{-1}. The Hawaiian results show that $v_x \sim$ 10 M - sec.$^{-1}$ (Fig. 16), $v_z \sim$ M - sec.$^{-1}$ (Fig. 17), Q $\sim 10^{-4}$ erg - M^{-3} - sec.$^{-1}$ (Fig. 18) and E $\sim$1 M - sec.$^{-1}$ (Fig. 15). The results show that the strongest thermal and dynamic responses in the thermosphere due to the magnetic storm are in the polar region and they become weaker as latitude decreases.

CHAPTER IV

CONCLUDING REMARKS AND RECOMMENDATIONS

In this study, a theoretical model for the dynamical responses to the geomagnetic storm in the thermosphere is derived from the magnetohydrodynamic theory. The validity of this proposed model is based on the assumption that the thermosphere behaves as an electric conducting fluid. This is true, because the degree of ionization in the thermosphere is $\sim 10^{-4}$ and thus, the dynamical properties in the thermosphere are dominated by the neutral gas. In order to test the proposed model. A numerical example is presented. In this calculation, we have neglected the viscous effects and fixed our attention only on a narrow region of the thermosphere, and constant transport properties are assumed in the model. In general, the results we obtained are in good agreement with the wind measurements from an Agena satellite [13] and joule heating obtained by Cole [3]. However, the calculated density and temperature in this model are unreasonably high. We believe this is because we have ignored the viscous effects, the altitude dependence, and the gravitational wave effects. Therefore, we shall recommend that this model be improved in the following manner:

1) By including the viscous effect.
2) By including a global calculation model using a suitable spherical coordinate system. Thus, the latitude dependence can be incorporated into the model.
3) Currently, our results are obtained for a point. We hope to do a calculation to include whole region of the atmosphere from 90 Km - 250 Km, the structure of the winds and electric field can be obtained.
4) By examining joule heating, the effects on gravitational wave.

These will form a basis of our future studies.

REFERENCES

(1) Chapman, S. and Bartel, J., Geomagnetism, Vols. I and II, Clarendon Press, Oxford, 1962.

(2) Piddington, J. S., Cosmic Electrodynamics, Wiley-Interscience Publication, John Wiley & Sons, Inc., New York, 1969.

(3) Cole, K. D., Australian J. Phys., Vol. 15, 1962, pp. 223-235.

(4) Cole, K. D., Planet. Space Sci., Vol. 19, 1971, pp. 59-75.

(5) Maeda, K. and Kato, S., Space Science Reviews 5, 1966, pp. 57-79.

(6) Thomas, G. E., Physics of Space Environment, edited by: Smith, R. E. and Wu, S. T., NASA SP-305, 1972, pp. 3-23.

(7) Thomas, G. E. and Ching, B. K., J. Geophys. Res., Vol. 74, 1969, pp. 1796-1811.

(8) Volland, H. and Mayer, H. G., J. Geophys. Res., Vol. 76, 1971, pp. 3764-3776.

(9) Chang, S. C., Wu, S. T., and Smith, R. E., URSI/COSPAR Symposium on "Dynamics of the Thermosphere and Ionosphere Above 120 KM," Seattle, Washington, 1971, C-4-8.

(10) Cowling, T. G., Proc. Roy. Soc., London, Vol. 183, 1945, p. 453.

(11) Piddington, J. H., Mon. Not. R. Astr. Soc. 114, 1954, pp. 651-663.

(12) Hartman, J. and Lazarus, F., Kgl. Danske, Videnskab, Selskab, Mat-Fys, Medal 15, 1937.

(13) Fees, W. F., URSI/COSPAR Symposium on "Dynamics of the Thermosphere and Ionosphere Above 120 KM," Seattle, Washington, 1971, C-1-6.

(14) Cole, K. D., Physics of Space Environment, edited by Smith, R. E. and Wu, S. T., NASA SP-305, 1972, pp. 25-38.

(15) Wu, S. T., Matsushita, S., and De Vries, L. L., "An Analysis of LOGACS Wind System," submitted for publication.

MHD MODEL OF THERMOSPHERE

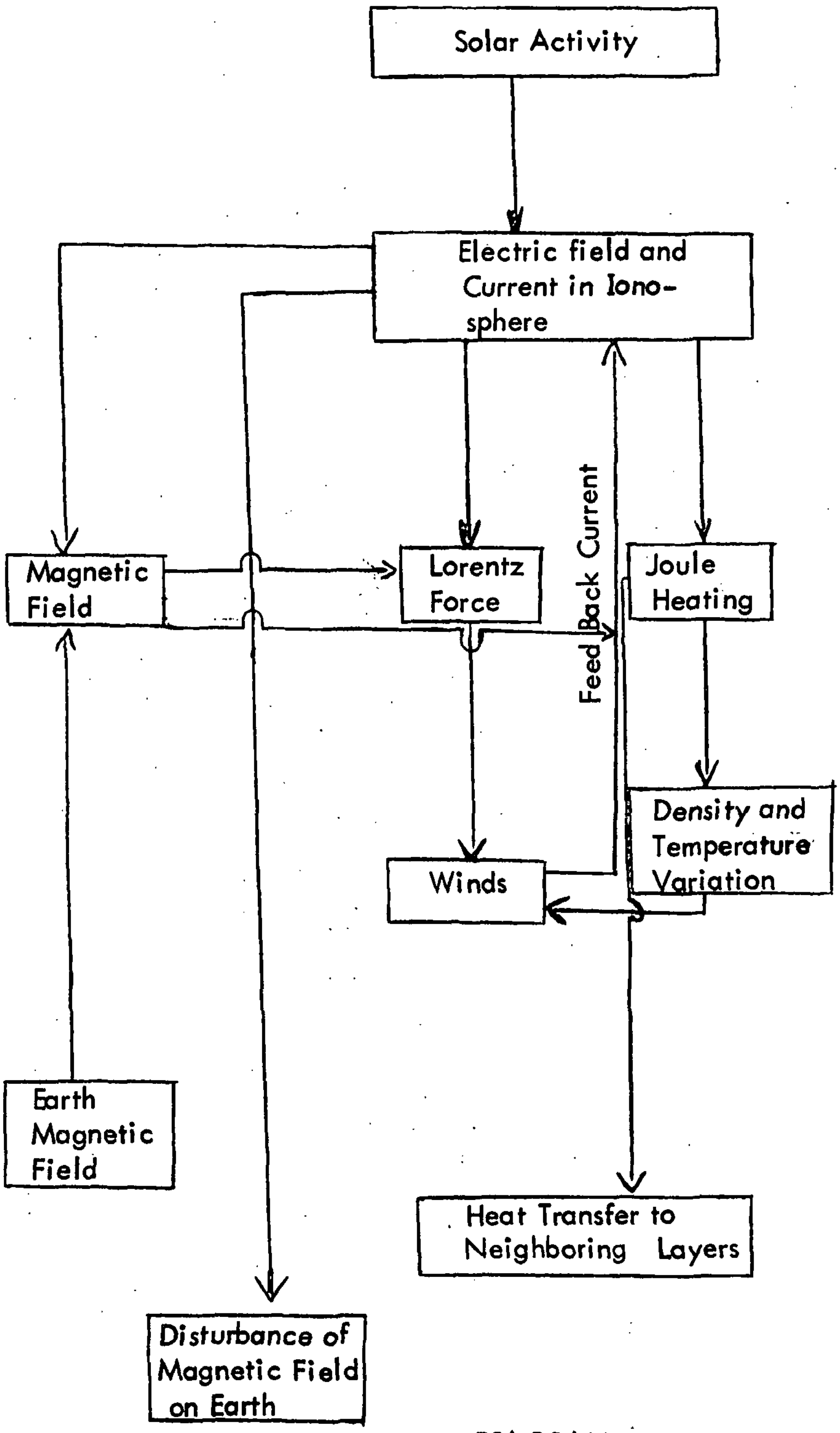

DIAGRAM I

$$\frac{\partial \rho}{\partial t} + \operatorname{div}(\rho \vec{V}) = 0 \qquad (1)$$

$$\frac{D\vec{V}}{Dt} = -\frac{1}{\rho}\operatorname{grad} p + \frac{1}{\rho}(\vec{j} \times \vec{B}) \qquad (2)$$

$$\rho\, c_p \frac{DT}{Dt} = \operatorname{div}(\lambda \operatorname{grad} T) + \vec{j} \cdot \vec{E}' \qquad (3)$$

$$\vec{E}' = \vec{E} + \vec{V} \times \vec{B} \qquad (4)$$

$$\operatorname{curl} \vec{E} = -\frac{\partial \vec{B}}{\partial t} \qquad (5)$$

$$\vec{j} = \sigma(\vec{E} + \vec{V} \times \vec{B}) = \sigma \vec{E}' \qquad (6)$$

$$p = \rho R T \qquad (7)$$

DIAGRAM II

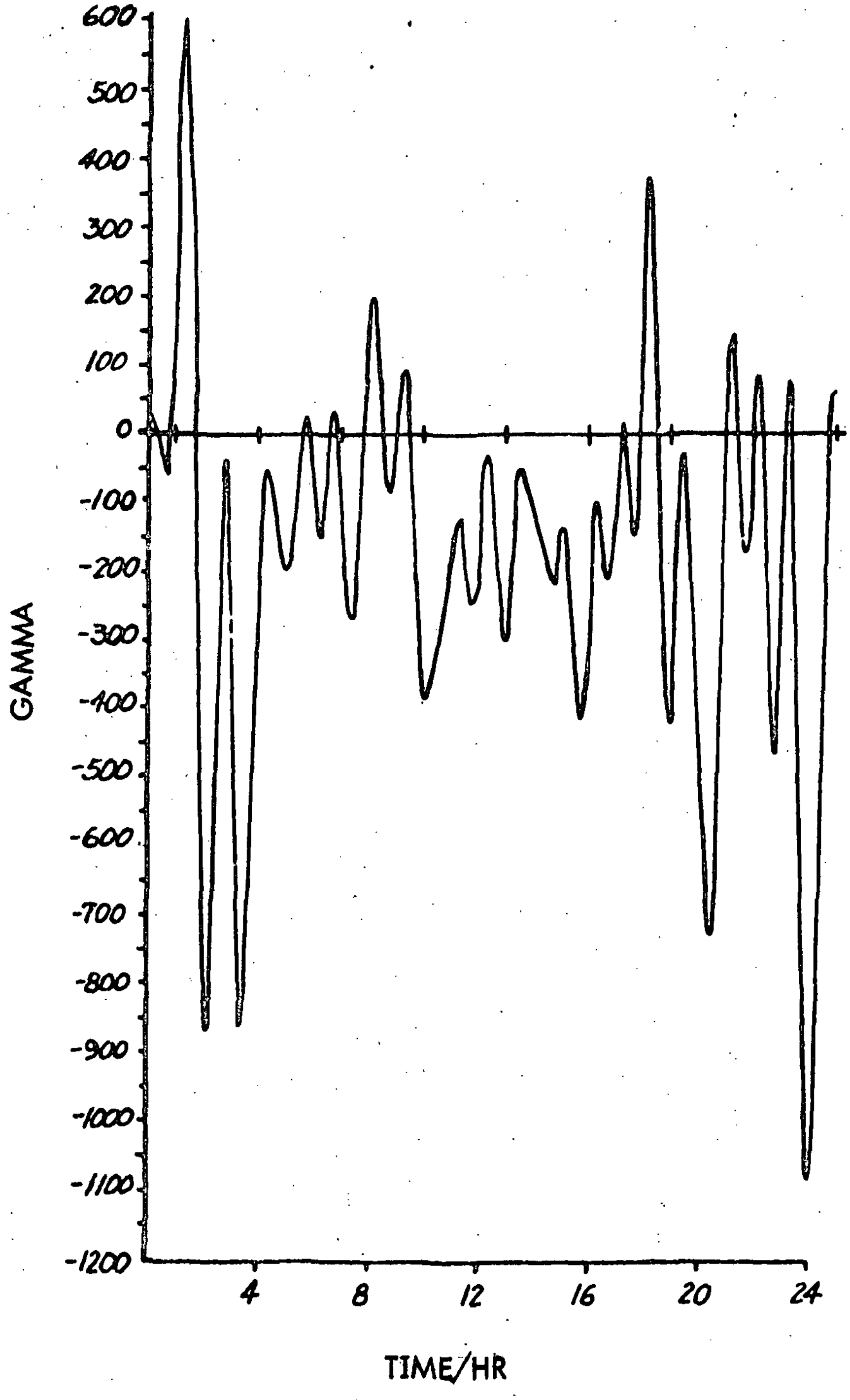
600
500
400
300
200
100
0
-100
-200
-300
-400
-500
-600
-700
-800
-900
-1000
-1100
-1200
GAMMA
4
8
12
16
20
24
TIME/HR

FIG. 1

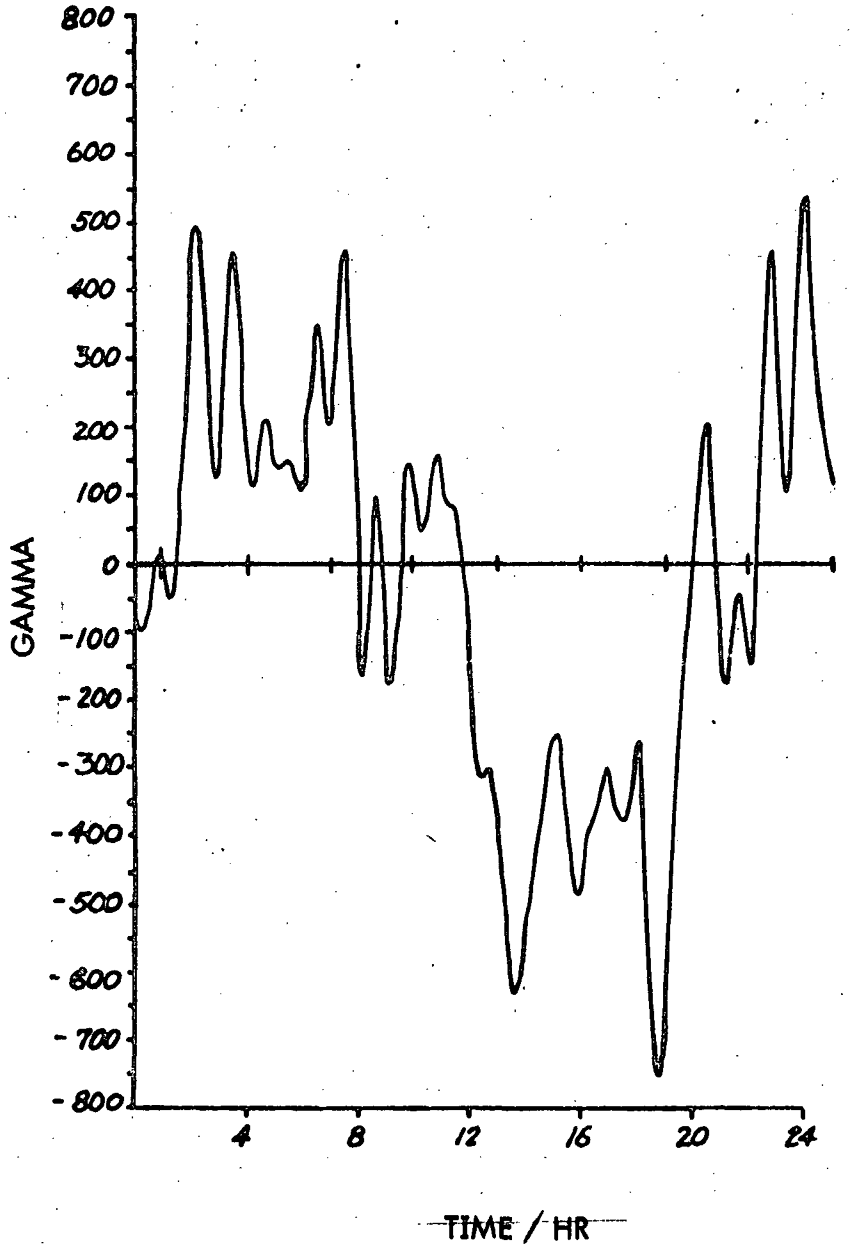
800
700
600
500
400
300
200
100
0
-100
-200
-300
-400
-500
-600
-700
-800
GAMMA
4
8
12
16
20
24
TIME / HR

FIG. 2

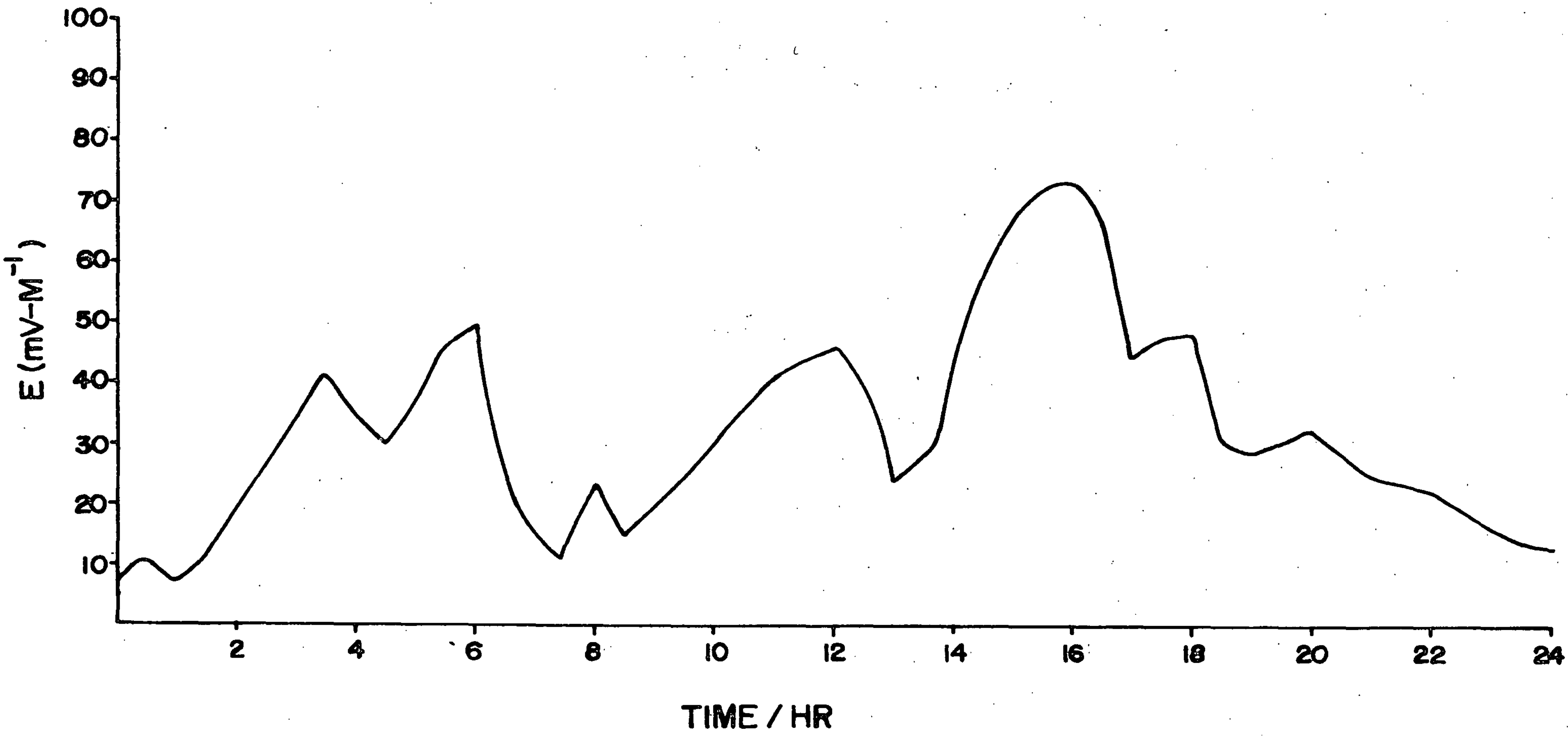
100
90
80
70
60
50
40
30
20
10
E (mV-M^{-1})
2
4
6
8
10
12
14
16
18
20
22
24
TIME / HR
FIG.3

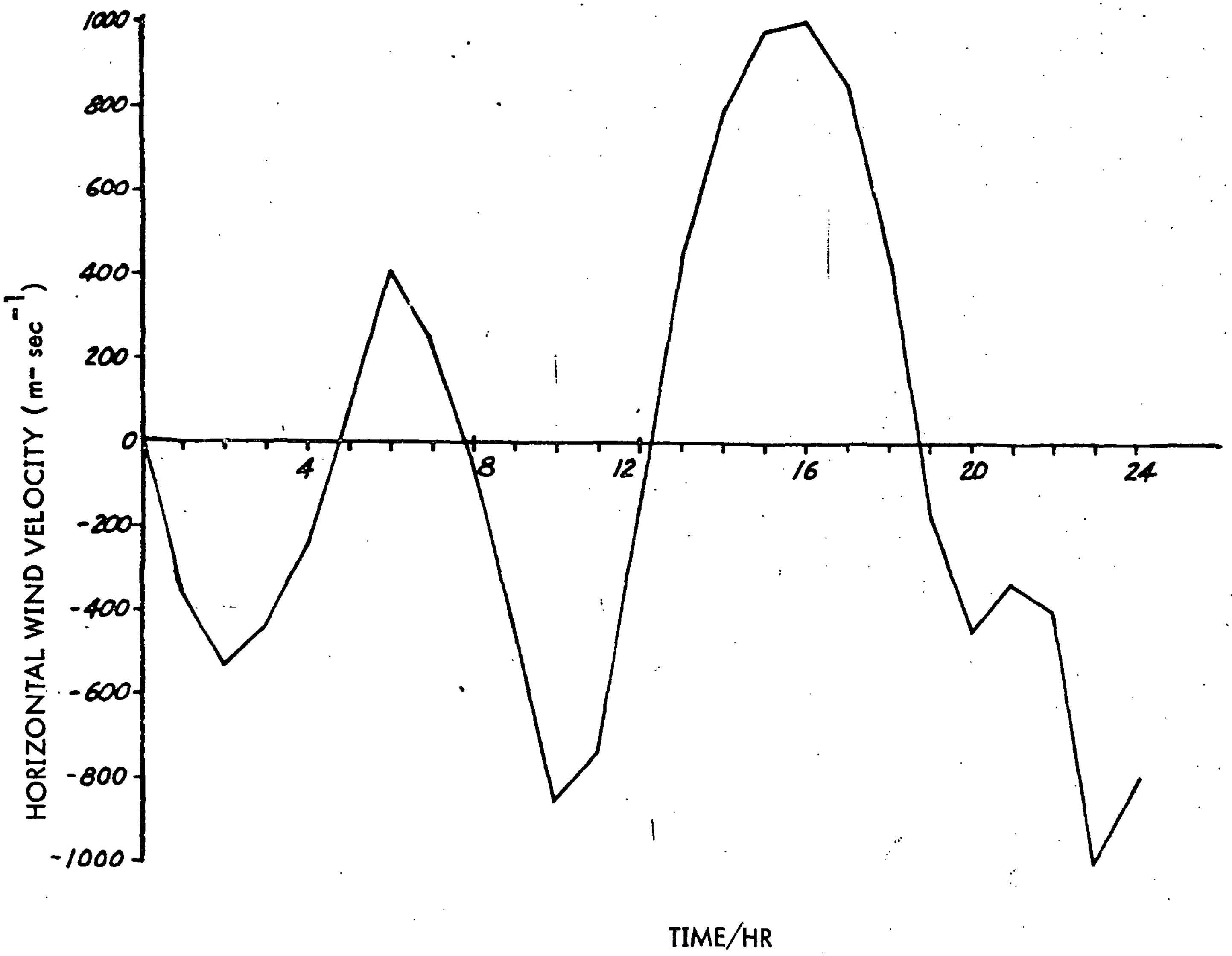
HORIZONTAL WIND VELOCITY (m- sec⁻¹)
1000
800
600
400
200
0
-200
-400
-600
-800
-1000
4
8
12
16
20
24
TIME/HR

FIG. 4

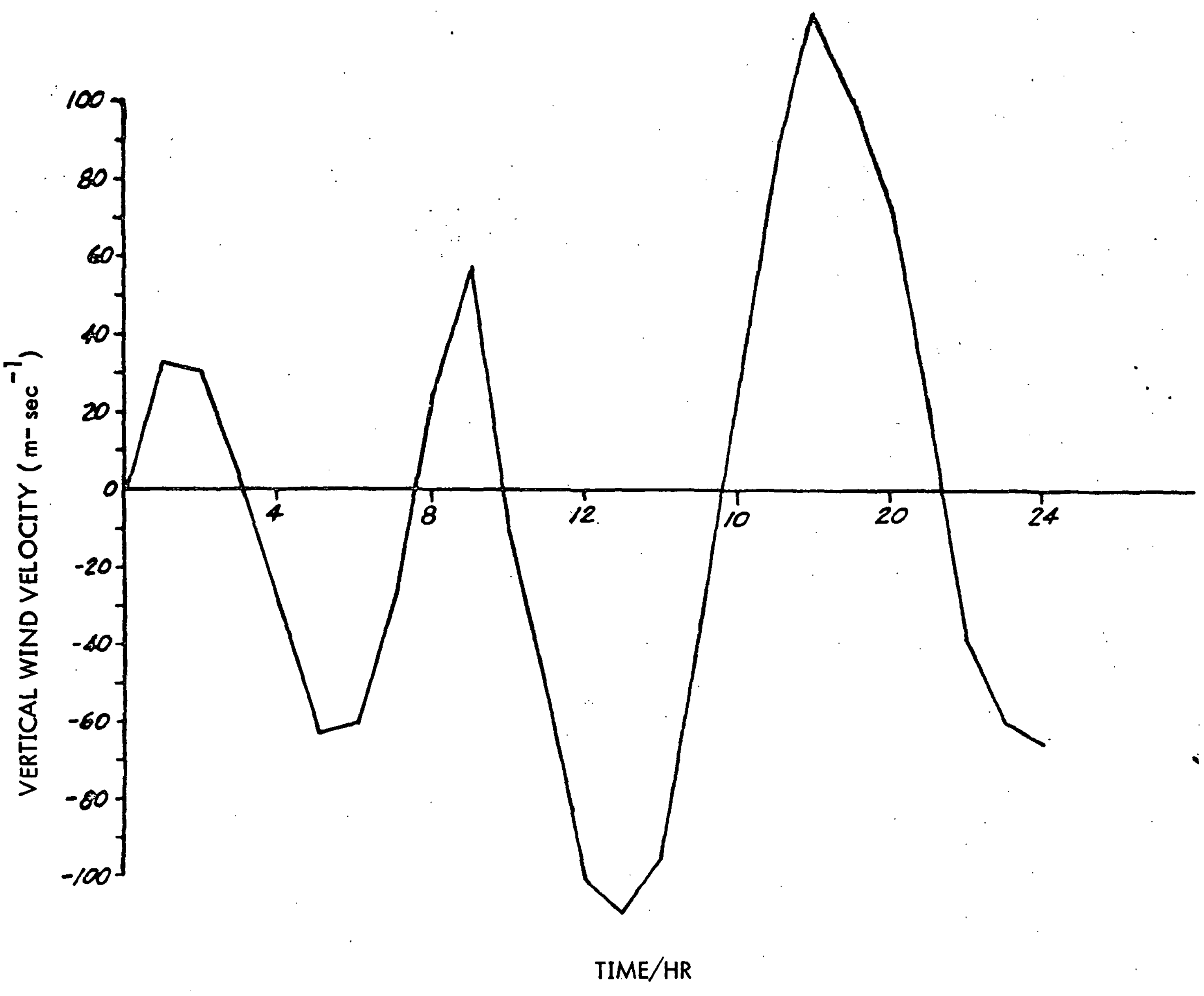
VERTICAL WIND VELOCITY (m- sec^{-1})
100
80
60
40
20
0
-20
-40
-60
-80
-100
4
8
12
10
20
24
TIME/HR

FIG. 5

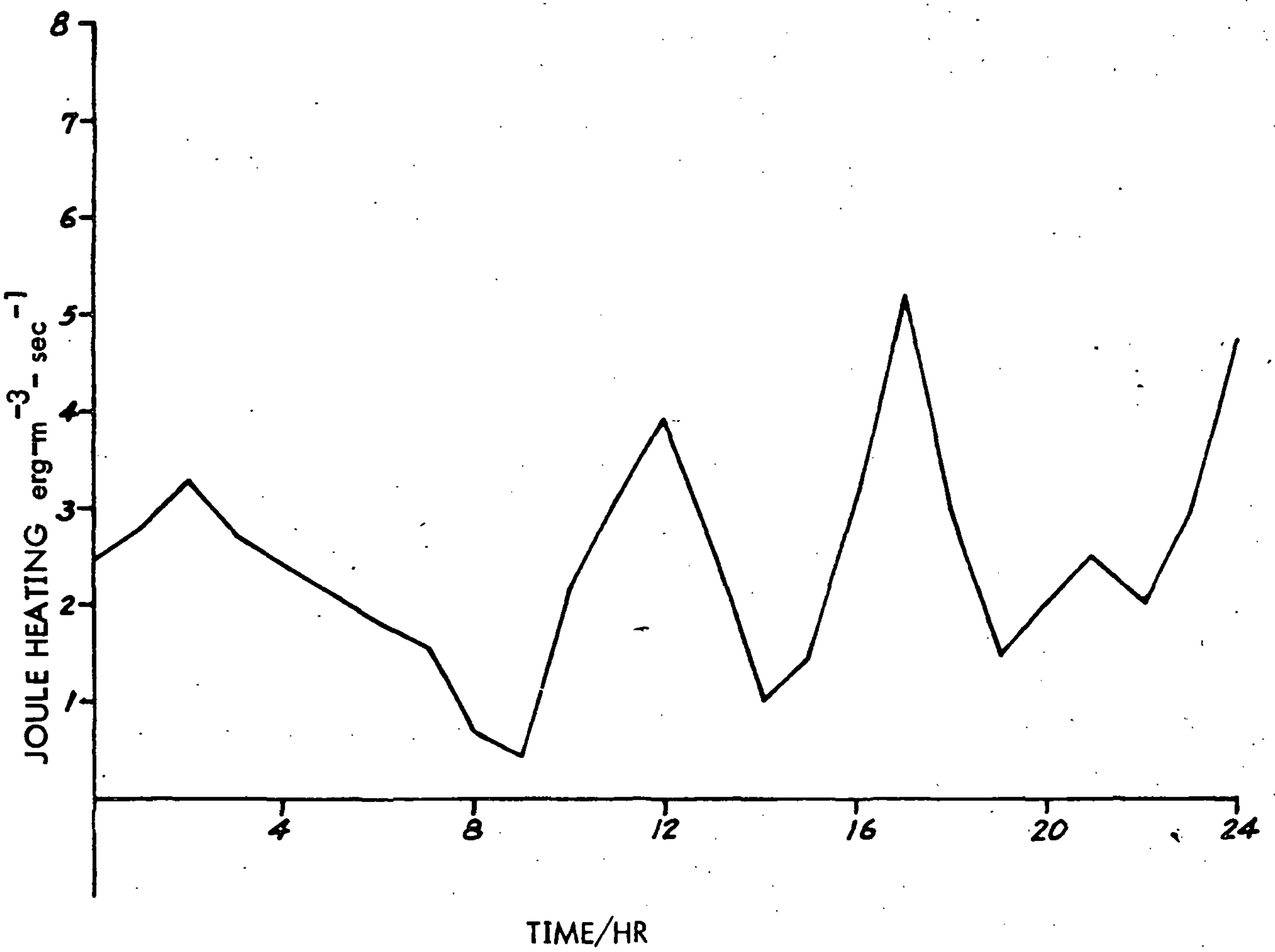

FIG. 6

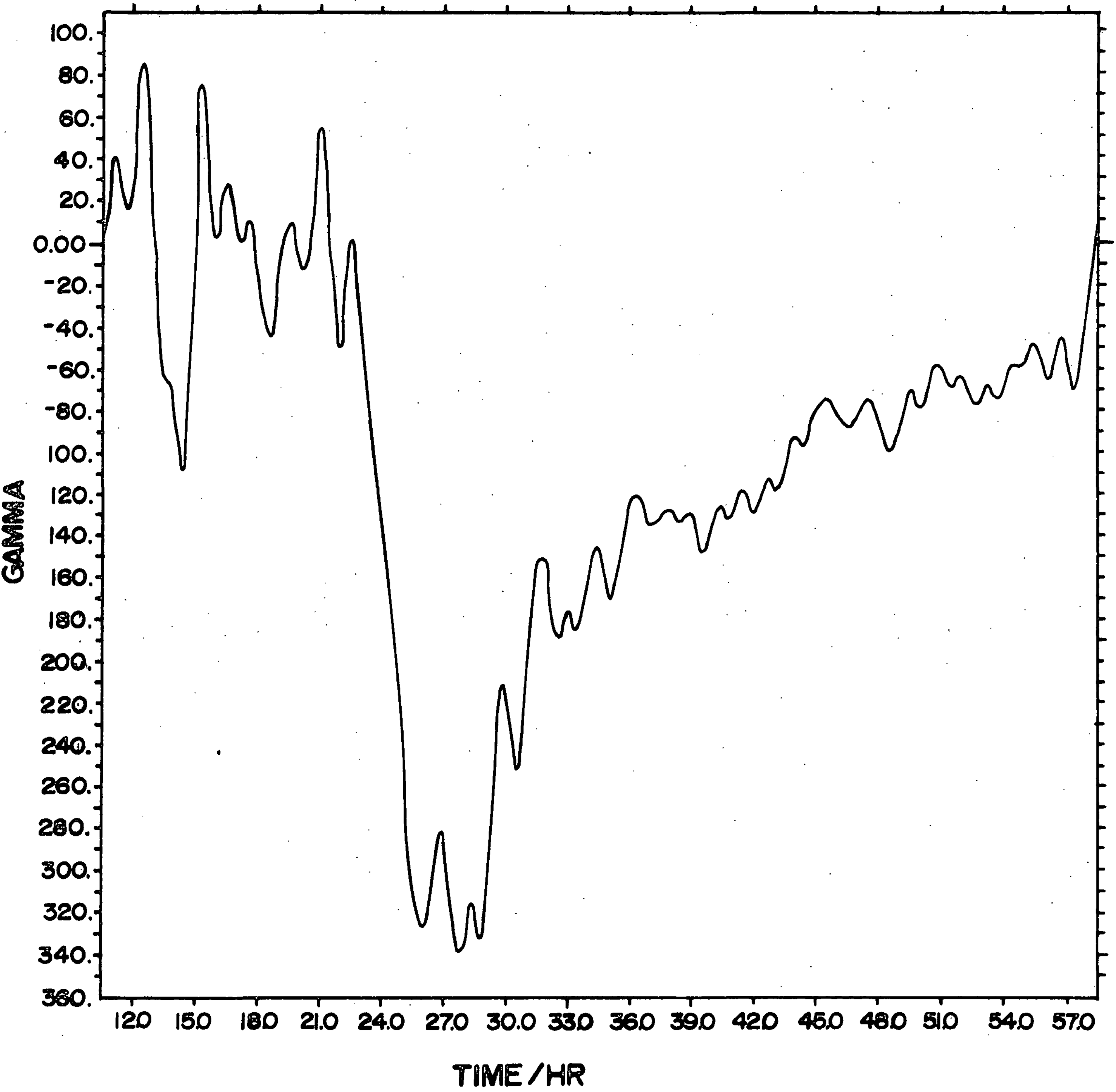
GAMMA
100.
80.
60.
40.
20.
0.00
-20.
-40.
-60.
-80.
100.
120.
140.
160.
180.
200.
220.
240.
260.
280.
300.
320.
340.
360.
12.0
15.0
18.0
21.0
24.0
27.0
30.0
33.0
36.0
39.0
42.0
45.0
48.0
51.0
54.0
57.0
TIME/HR

Fig. 7

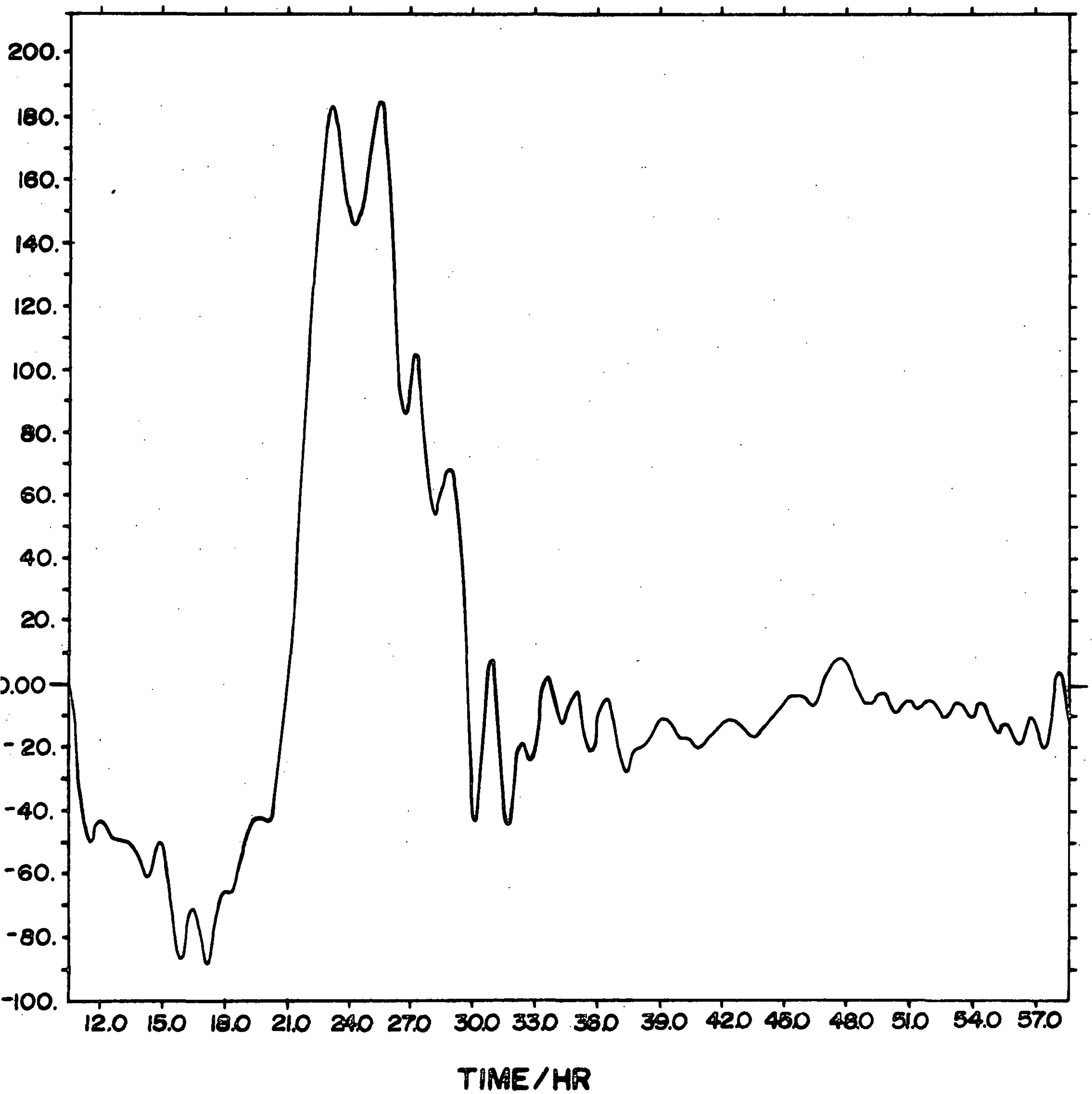

200.
180.
160.
140.
120.
100.
80.
60.
40.
20.
0.00
-20.
-40.
-60.
-80.
-100.
12.0 15.0 18.0 21.0 24.0 27.0 30.0 33.0 36.0 39.0 42.0 45.0 48.0 51.0 54.0 57.0
TIME/HR

Fig. 8

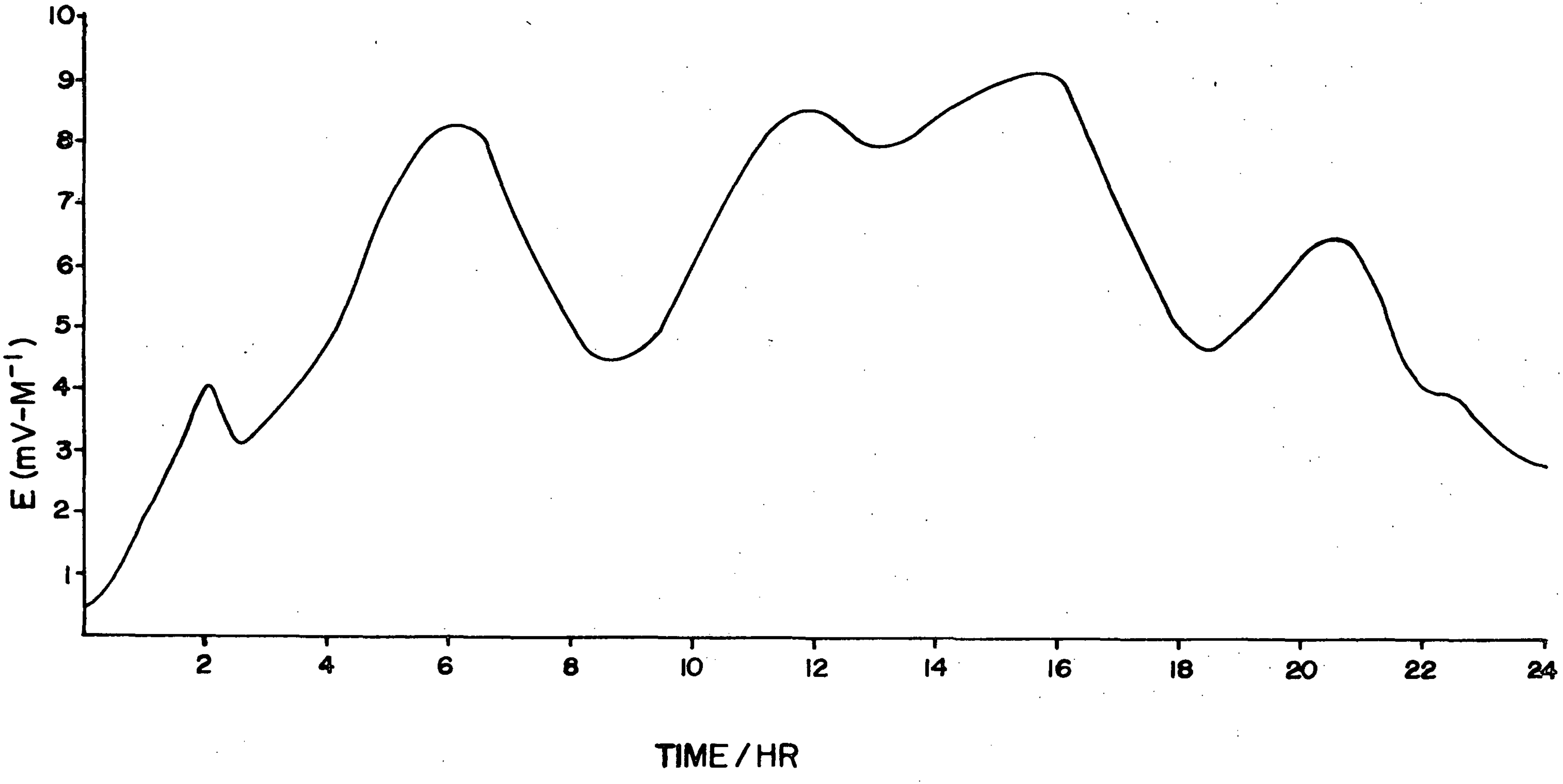

FIG. 9

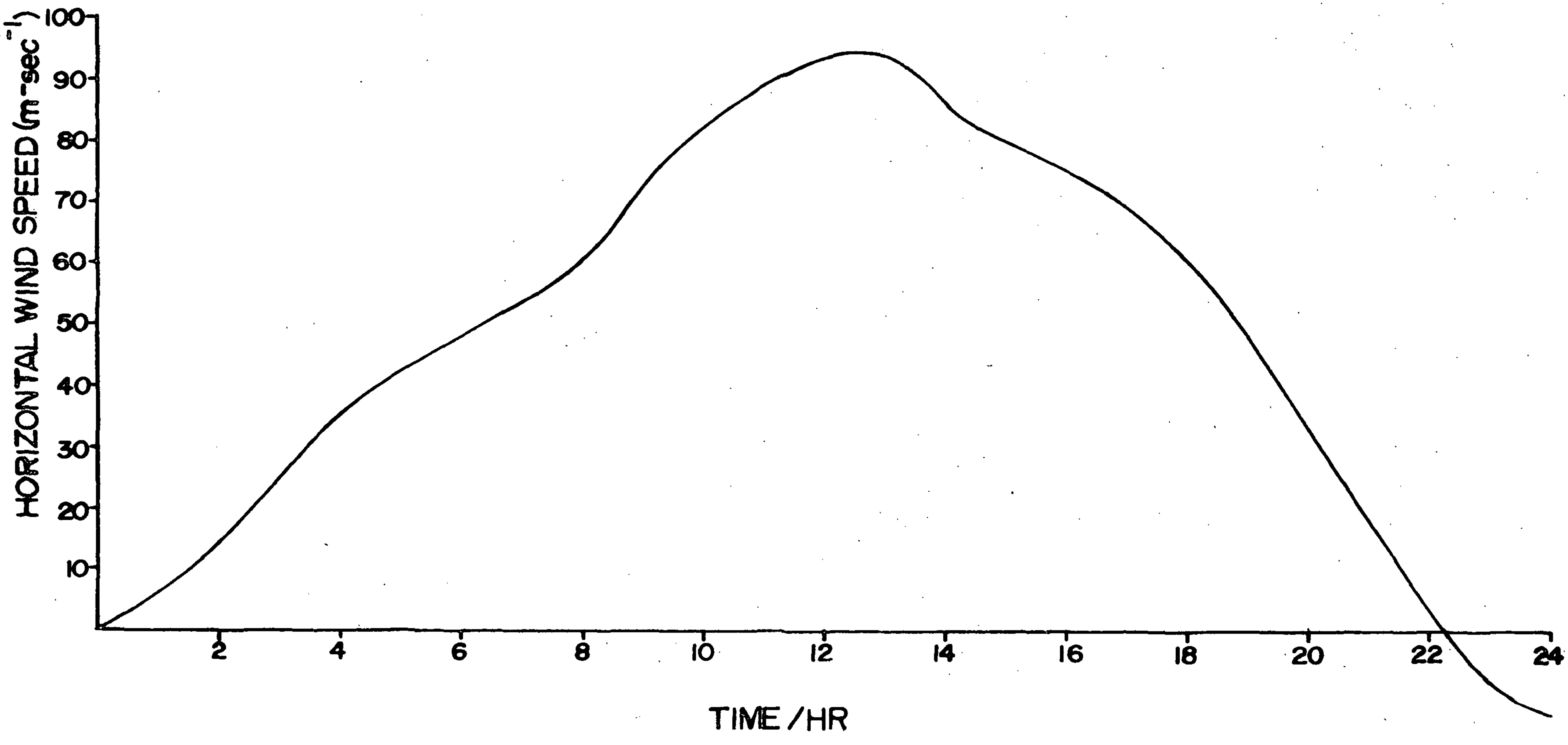
HORIZONTAL WIND SPEED (m-sec^{-1})
100
90
80
70
60
50
40
30
20
10
2
4
6
8
10
12
14
16
18
20
22
24
TIME / HR

Fig. 10

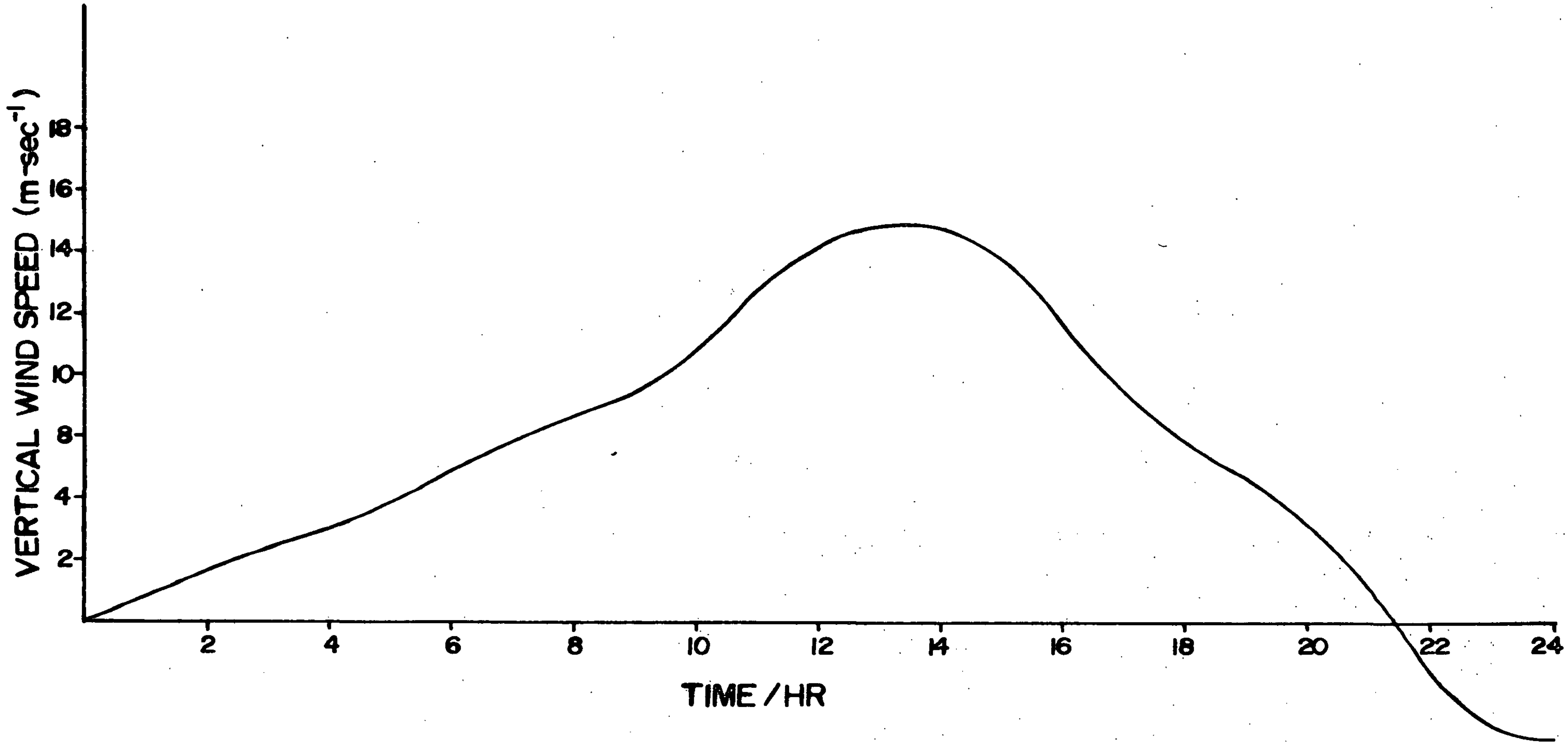
VERTICAL WIND SPEED (m-sec^{-1})
18
16
14
12
10
8
4
2
2
4
6
8
10
12
14
16
18
20
22
24
TIME / HR

Fig. 11

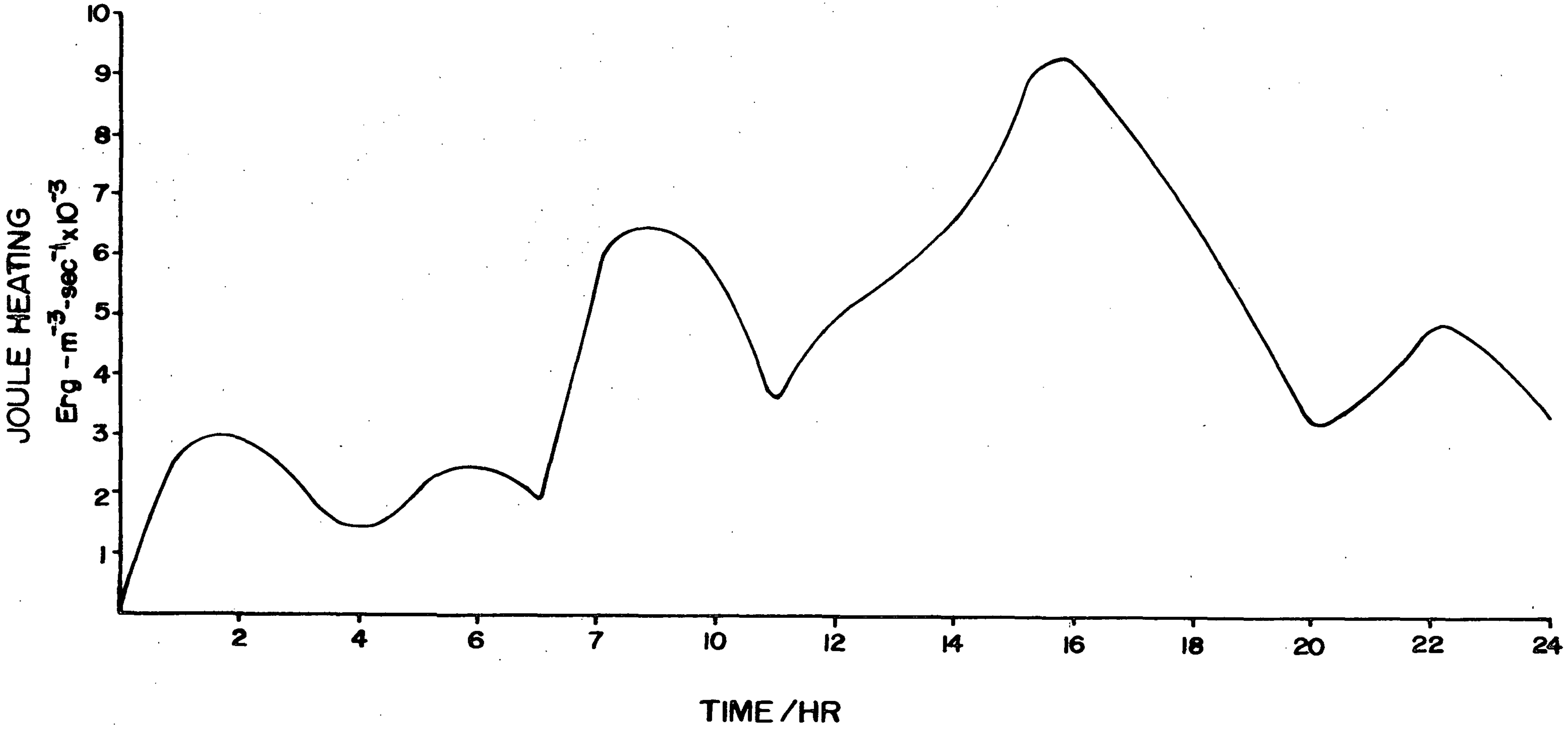
JOULE HEATING
Erg - m^{-3}-sec^{-1} x 10^{-3}
10
9
8
7
6
5
4
3
2
1
2
4
6
7
10
12
14
16
18
20
22
24
TIME / HR

Fig. 12

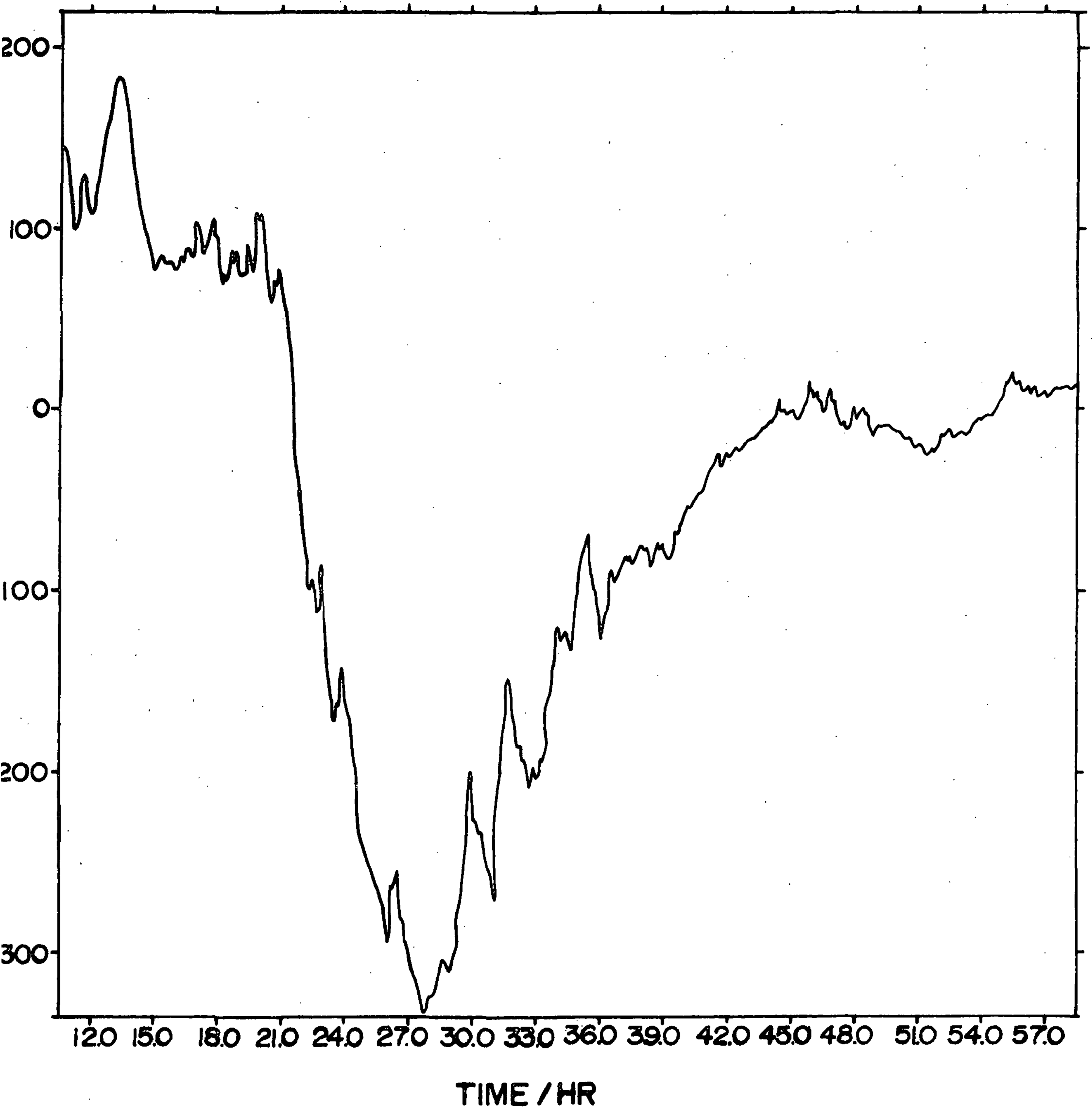
200
100
0
100
200
300
12.0 15.0 18.0 21.0 24.0 27.0 30.0 33.0 36.0 39.0 42.0 45.0 48.0 51.0 54.0 57.0
TIME / HR

FIG. 13

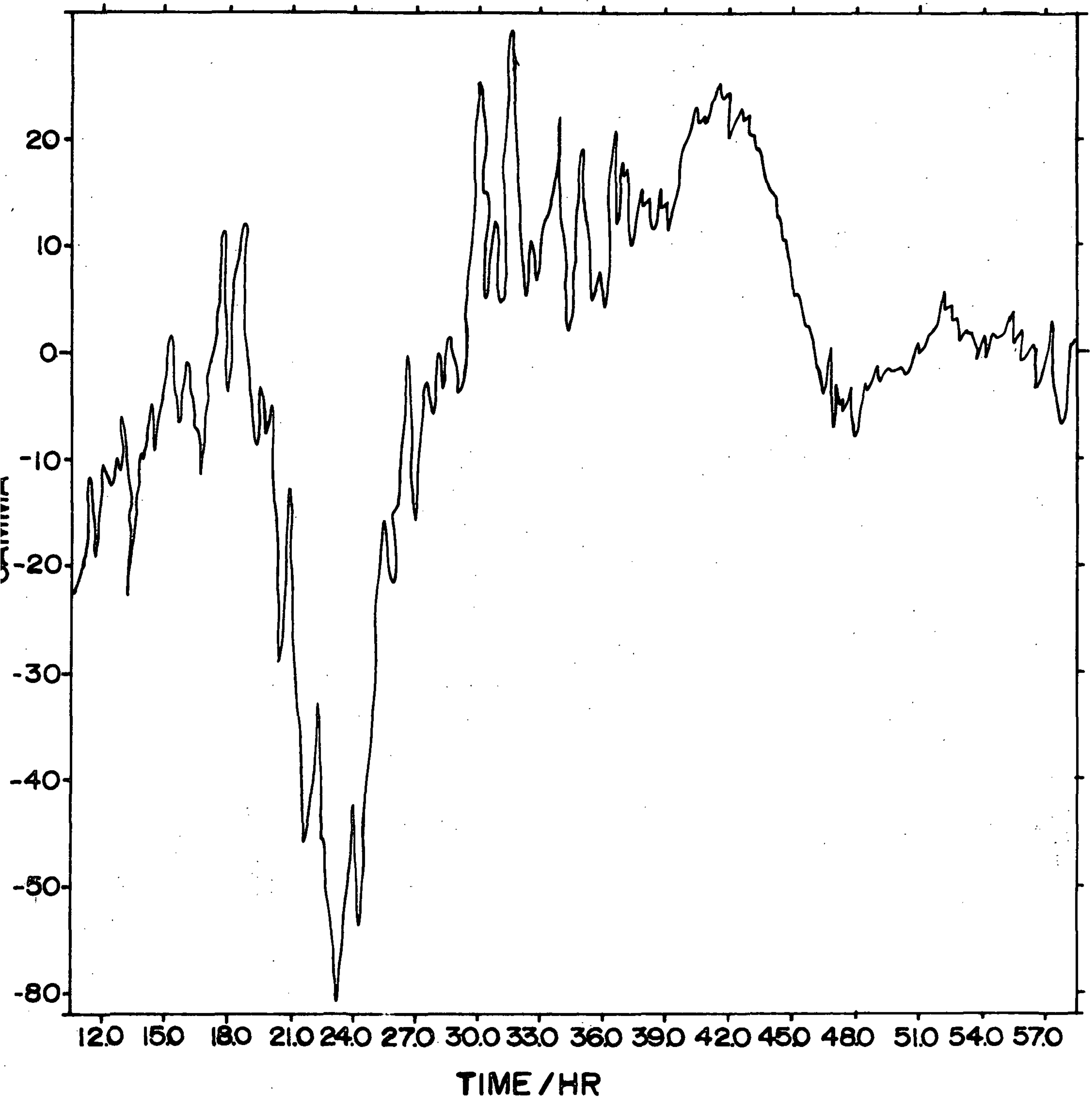
20
10
0
-10
-20
-30
-40
-50
-80
12.0 15.0 18.0 21.0 24.0 27.0 30.0 33.0 36.0 39.0 42.0 45.0 48.0 51.0 54.0 57.0
TIME / HR

FIG. 14

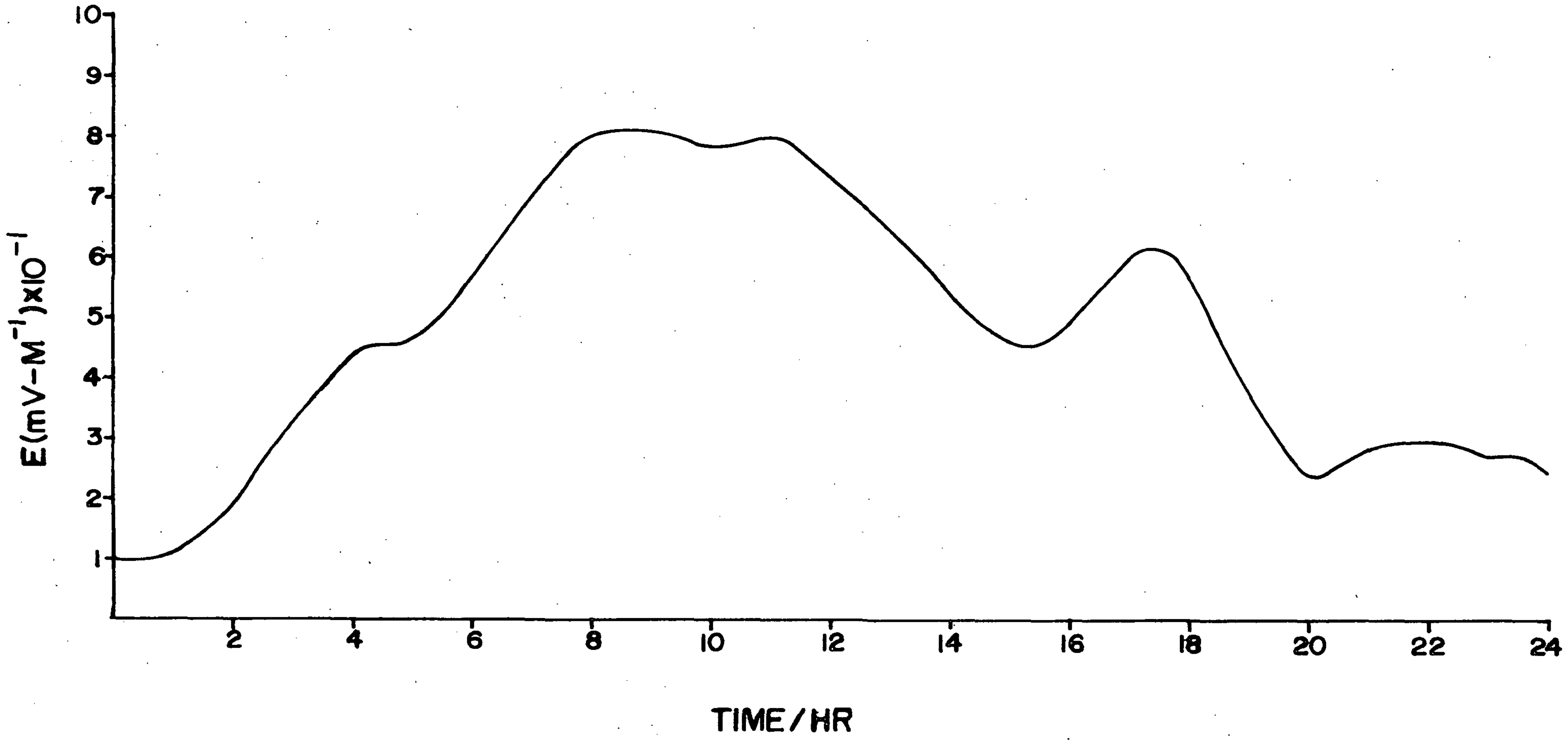

FIG. 15

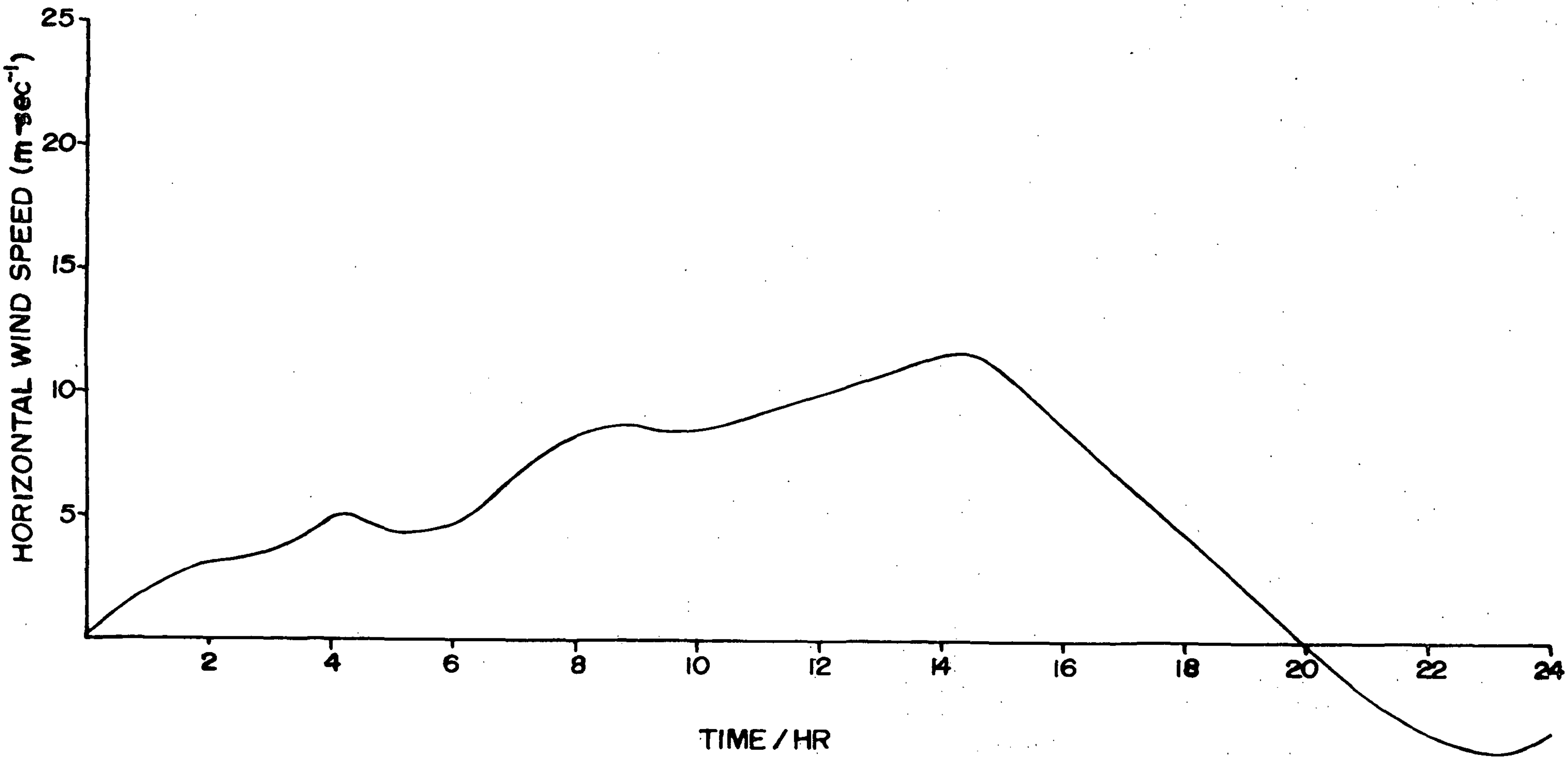

HORIZONTAL WIND SPEED (m sec^{-1})
25
20
15
10
5
2
4
6
8
10
12
14
16
18
20
22
24
TIME / HR

FIG. 16

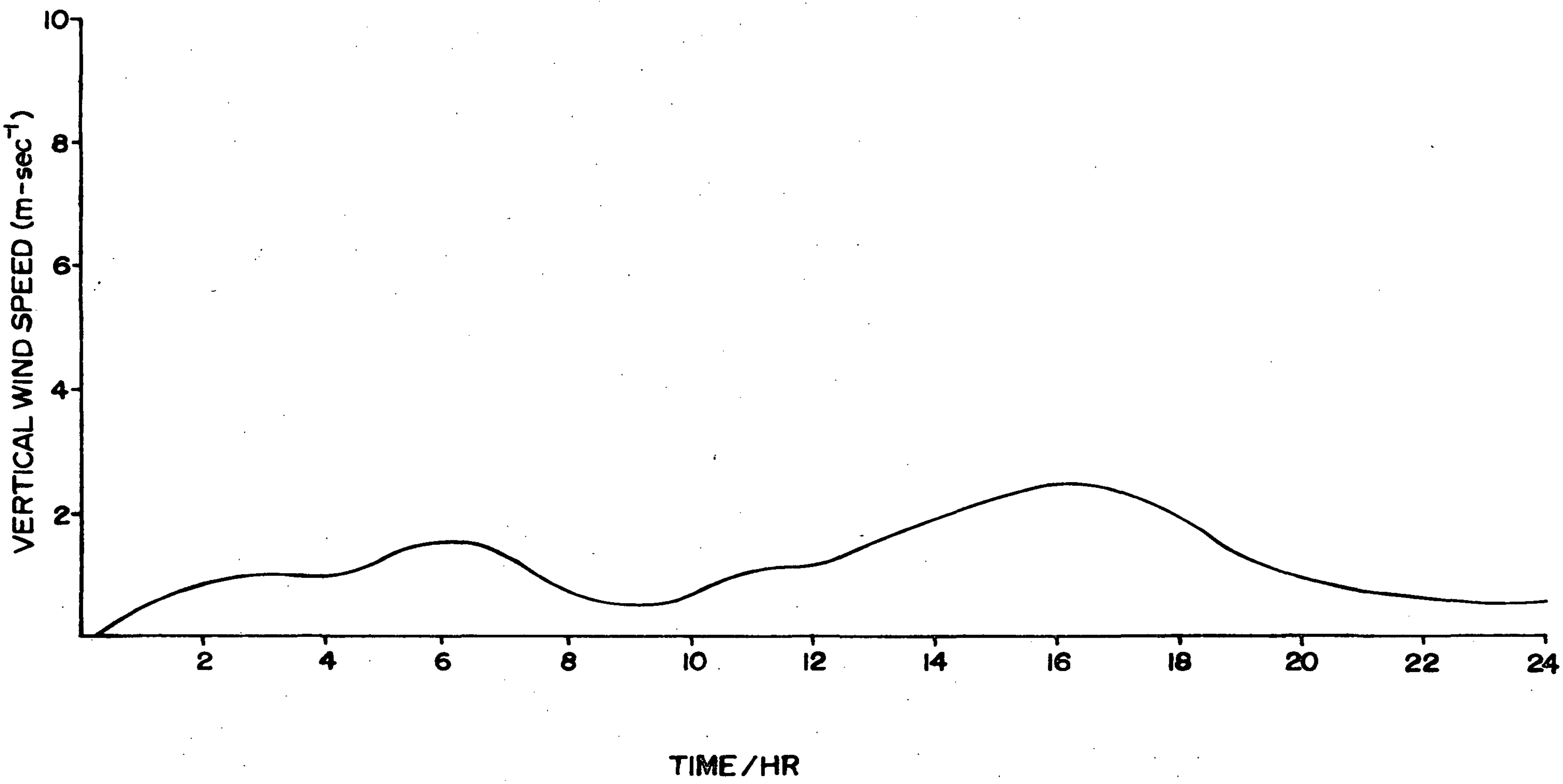
VERTICAL WIND SPEED (m-sec^{-1})
10
8
6
4
2
2
4
6
8
10
12
14
16
18
20
22
24
TIME/HR

FIG. 17

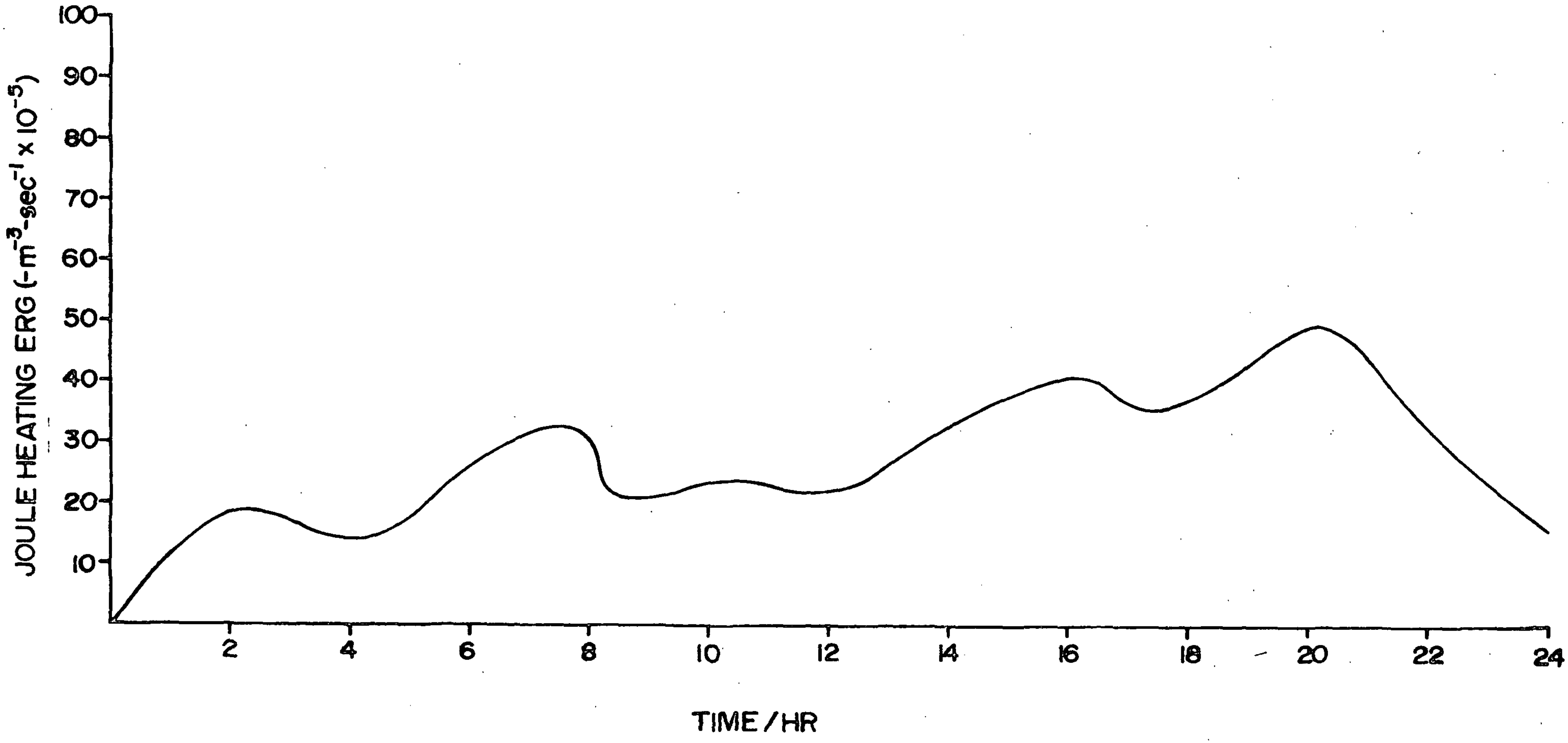
JOULE HEATING ERG (-m^-3-sec^-1 x 10^-5)
100
90
80
70
60
50
40
30
20
10
2
4
6
8
10
12
14
16
18
20
22
24
TIME / HR

FIG. 18